E. 結論

in vitro BBB モデルにミクログリアを添加することで健常脳から病態脳まで網羅したモデルとなり得ることが示唆された。また、ミクログリアによる barrier function の制御にサイトカイン、ケモカインが関与していることが示された。

F. 研究発表

1. 論文発表

1. Fujimori K, Takaki J, Miura M, Shigemoto-Mogami Y, Sekino Y, Suzuki T, Sato K, Paroxetine prevented the down-regulation of astrocytic L-Glu transporters in neuroinflammation, J Pharamcol Sci (in press)
2. Shigemoto-Mogami Y, Fujimori K, Ikarashi Y, Hirose A, Sekino Y, Sato K, Residual metals in carbon nanotubes suppress the proliferation of neural stem cells. (2014) Fundam Toxcol Sci, 1(3), 87-94 (2014)
3. Shigemoto-Mogami Y, Hoshikawa K, Goldman JE, Sekino Y, Sato K, (2014) Microglia enhance neurogenesis and oligodendrogenesis in the early postnatal subventricular zone. J Neurosci 34(5), 2231-2243
4. Fujieda T, Koganezawa N, Ide Y, Shirao T, Sekino Y, An inhibitory pathway controlling the gating mechanism of the mouse lateral amygdala revealed by voltage-sensitive dye imaging. (2015) Neurosci Lett. 590C:126-131. doi: 10.1016/j.neulet. 2015.01.079
5. Nagakubo T, Demizu Y, Kanda Y,

Misawa T, Shoda T, Okuhira K, Sekino Y, Naito M, Kurihara M, Development of Cell-Penetrating R7 Fragment -Conjugated Helical Peptides as Inhibitors of Estrogen Receptor-Mediated Transcription. (2014) Bioconjug Chem. 25(11): 1921-1924

6. Hirata N., Yamada S., Shoda T. ,Kurihara M., Sekino Y., Kanda Y, Sphingosine-1-phosphate promotes expansion of cancer stem cells via S1PR3 by a ligand-independent Notch activation. Nat Common. 5: 4806. doi: 10.1038/ncomms5806. (2014)
7. Kim SR, Kubo T, Hojyo M, Matsuo T, Miyajima A, Usami M, Sekino Y, Matsushita T, Ishida S, Comparative metabolome analysis of cultured fetal and adult hepatocytes in human. (2014) J Toxicol Sci. 39(5): 717-723
8. Yamada S, Kotake Y, Demizu Y, Kurihara Y, Sekino Y, Kanda Y, NAD-dependent isocitrate dehydrogenase as a novel target of tributyltin in human embryonic carcinoma cells. (2014) Sci. Rep. 4: 5952. doi: 10.1038/srep05952
9. Nakamura Y, Matsuo J, Miyamoto N, Ojima A, Ando K, Kanda Y, Sawada K, Sugiyama A, Sekino Y, Assessment of testing methods for drug-induced repolarization delay and arrhythmias in an iPS cell-derived cardiomyocyte sheet: multi-site validation study. (2014) J Pharmacol Sci. 124(4): 494-501
10. Ishikawa M, Shiota J, Ishibashi Y, Hakamata T, Shoji S, Fukuchi M, Tsuda M, Shirao T, Sekino Y. Baraban JM, Tabuchi A Cellular localization and dendritic function of rat isoforms of the SRF coactivator MKL1 in cortical neurons. (2014) Neuroreport. 25(8): 585-592
11. Yamazaki H, Kojima N, Kato K, Hirose H, Iwasaki T, Mizui T, Takahashi H, Hanamura K, Roppongi RT, Koibuchi N, Sekino Y, Mori N, Shirao T, Spikar, a novel drebrin-binding protein, regulates the formation and stabilization of dendritic spines. (2014) J Neurochem. 128(4): 507-522
12. Mizui T, Sekino Y, Yamazaki Y, Ishizuka H, Takahashi H, Kojima N, Kojima M, Shirao T, Myosin II ATPase activity mediates the long-term potentiation-induced exodus of stable F-actin bound by drebrin A from dendritic spines. (2014) PLOS ONE. 9(1) e8536722
13. Irie T, Matsuzaki Y, Sekino Y, Hirai H, Kv3.3 channels harboring

a mutation of spinocerebellar ataxia type 13 alter excitability and induce cell death in cultured cerebellar Purkinje cells. (2014) J Physiol. 592(Pt1) 34: 229-247

2. 学会発表

【国内学会】

1. 関野　祐子、ヒト iPS 細胞由来組織細胞を用いた化学物質の安全性評価法の開発、日本化学会秋季事業第４回　CSJ 化学フェスタ 2014（2014.10）（東京）
2. 関野　祐子、ヒト iPS 細胞由来心筋細胞を用いた新規安全性薬理試験法の開発と評価、第５８回日本薬学会関東支部大会　ランチョンセミナー（2014.10）（東京）
3. 関野　祐子、ヒト iPS 細胞由来細胞を用いた安全性薬理学の新たな展望、第 21 回 HAB 研究機構学術年会（2014.5）（東京）
4. 関野　祐子、h-iPS 由来神経細胞を利用した薬理試験法開発の現状と課題、第 7 回上肢の神経機能回復セミナー（2014.5）（秋田）
5. 佐藤　薫、高橋 華奈子、最上（重本） 由香里、金村米博、正札智子、福角 勇人、岡田 洋平、岡野 栄之、白尾 智明、関野 祐子、興奮毒性評価が可能なヒト iPS 細胞由来神経細胞を用いた薬理試験系確立の試み、第 88 回　日本薬理学会年会（2015.3）（名古屋）
6. 最上（重本） 由香里、 干川 和枝、関野　祐子、佐藤　薫、ミクログリアの活性状態に依存した血液脳関門のバリア機能への影響、日本薬学会　第 135 年会 (2015.3)（神戸）
7. 佐藤　薫、高橋 華奈子、最上（重本） 由香里、金村 米博、正札 智子、福角 勇人、岡田 洋平、岡野 栄之、白尾 智明、関野 祐子、興奮毒性評価が可能なヒト iPS 細胞由来神経細胞の探索、日本薬学会　第 135 年会（2015.3）（神戸）
8. 高橋 華奈子、最上(重本) 由香里、中條 かおり、干川 和枝、金村 米博、正札 智子、福角 勇人、岡田 洋平、岡野 栄之、白尾 智明、関野 祐子、佐藤　薫、ヒト人工多能性幹細胞由来神経細胞の非臨床試験への応用の試み、第 14 回　日本再生医療学会総会（2015.3）（横浜）
9. Sato K, Takahashi K, Shigemoto-Mogami Y, Kanemura Y, Shofuda T, Fukusumi H, Okada Y, Okano H, Shirao T, Sekino Y, An attempt to establish neuron-specific toxicity evaluation systems using human iPSC-derived neurons, 日本安全性

薬理研究会第 6 回学術年会 (2015.2) (東京)

10. Sato K, Takahashi K, Shigemoto-Mogami Y, Kanemura Y, Shofuda T, Fukusumi Y, Okada Y, Okano H, Shirao T, Sekino Y, An attempt to establish non-clinical experiments for nervous system using human iPSC-derived neurons, The 18th Takeda science foundation symposium on bioscience 'iPS Cells for regenerative medicine' (2015.1) (Osaka)
11. Takahashi K, Shigemoto-Mogami Y, Ohtsu K, Okada Y, Okano H, Sekino Y, Sato K, Establishment of neuron-specific toxicity evaluation system using human induced pluripotent stem cell-derived neurons, CBI 学会 2014 年大会 (2014.10) (東京)
12. Sato K, Shigemoto-Mogami Y, Hoshikawa K, Goldman JE, Sekino Y, Discovery of the population of activated microglia which enhance neurogenesis and oligodendrogenesis in the early posnatal subventricuar zone, Neuroscience2014 (2014.9) (Yokohama)
13. Takahashi K, Shigemoto-Mogami Y, Ohtsu K, Okada Y, Okano H, Sekino Y, Sato K, Application of human induced pluripotent stem cell-derived neurons to the neurotoxicity evaluation system, Neuroscience2014 (2014.9) (Yokohama)
14. Shigemoto-Mogami Y, Hoshikawa K, Sekino Y, Sato K, Development of in vitro blood-brain barrier model including microglia, Neuroscience2014 (2014.9) (Yokohama)
15. Kasahara Y, Fujimori K, Miura M, Mogami Y, Sekino Y, Sato K, Suzuki T, Comparison of the effects of antidepressants on the microglial activation in LPS-inflammation model, Neuroscience2014 (2014.9) (Yokohama)
16. Roppongi RT, Ohara Y, Koganezawa N, Yamazaki H, Ootsu M, Sato K, Sekino Y, Shirao T, Slow axonal growth in human iPSCs-derived neurons, Neuroscience2014 (2014.9) (Yokohama)
17. Sato K, Takahashi K, Shigemoto-Mogami Y, Ohtsu K, Kanemura Y, Shofuda T, Fukusumi H, Okada Y, Okano H, Sekino Y, An attempt to apply human induced pluripotent stem cell-derived neurons to the

excitotoxicity evaluation system, 第 36 回　日本生物学的精神医学会・第 57 回　日本神経化学会大会合同大会（2014.9）（奈良）

18. Otsu M, Yamazaki H, Roppongi RI, Koganezawa N, Ohara Y, Sato K, Sekino Y, Shirao T, Application of human iPSC-derived neurons at early developmental stages for drug discovery, 第 36 回　日本生物学的精神医学会・第 57 回　日本神経化学会大会合同大会（2014.9, 奈良）

【国際学会】

1. Sekino Y, JiCSA Study Data Review (JiCSA 研究データのまとめ) CIPA Update Workshop CSRC-HESI-SPS-FDA Meeting (2014.12) (Maryland, USA)
2. Sekino Y. Human iPS-derived cardiomyocyte for development of in vitro pre-clinical testing（ヒト iPS 由来心筋細胞を用いたインビトロ前臨床試験の開発）ILSI HESI、Stem cell-derived Cardiomyocytes as Model of Cardiac Pathology and Toxicity Workshop (2013.3) (Cambridge, USA)
3. Sato K, Shegemoto-Mogami Y, Hoshikawa K, Sekino Y, Microglia accelerate the maturation of barrier function of blood brain barrier, SfN2014 (2014.11) (Washington D.C., USA)
4. Koganezawa K, Ohara Y, Yamazaki H, Roppongi RI, Sato K, Sekino Y, Shirao T, Axonal polarity formation in human iPSCs-derived neurons, SfN2014 (2014.11) (Washington D.C., USA)
5. Sato K, Takahashi K, Shigemoto-Mogami Y, Ohtsu K, Kanemura Y, Shofuda T, Fukusumi H, Okada Y, Okano H, Shirao T, Sekino Y, Sato K, Search for the human induced pluripotent stem cell-derived neurons capable of detecting the CNS-specific toxicity, SPS 14th annual meeting (2014.10) (Washington D.C., USA)
6. Sekino Y, Ootsu M, Ohara Y, Yamazaki H, Sato K, Roppongi R, Koganezawa N, Shirao T, Effects of valproic acid and astemizole on the neurite growth of human iPSCs-derived neurons, SPS 14th annual meeting (2014.10) (Washington D.C., USA)
7. Sato K, Shigemoto-Mogami Y, Hoshikawa K, Goldman JE, Sekino Y, The Discovery of a Population of Microglia Which Enhance Neurogenesis and Oligodendrogenesis in the Early

Postnatal SVZ, 9th FENS forum of neuroscicence (2014.7) (Milan, Italy)

G. 知的財産権の出願・登録状況

1. 特許取得　　なし
2. 実用新案登録　なし
3. その他　　なし

Figure 1

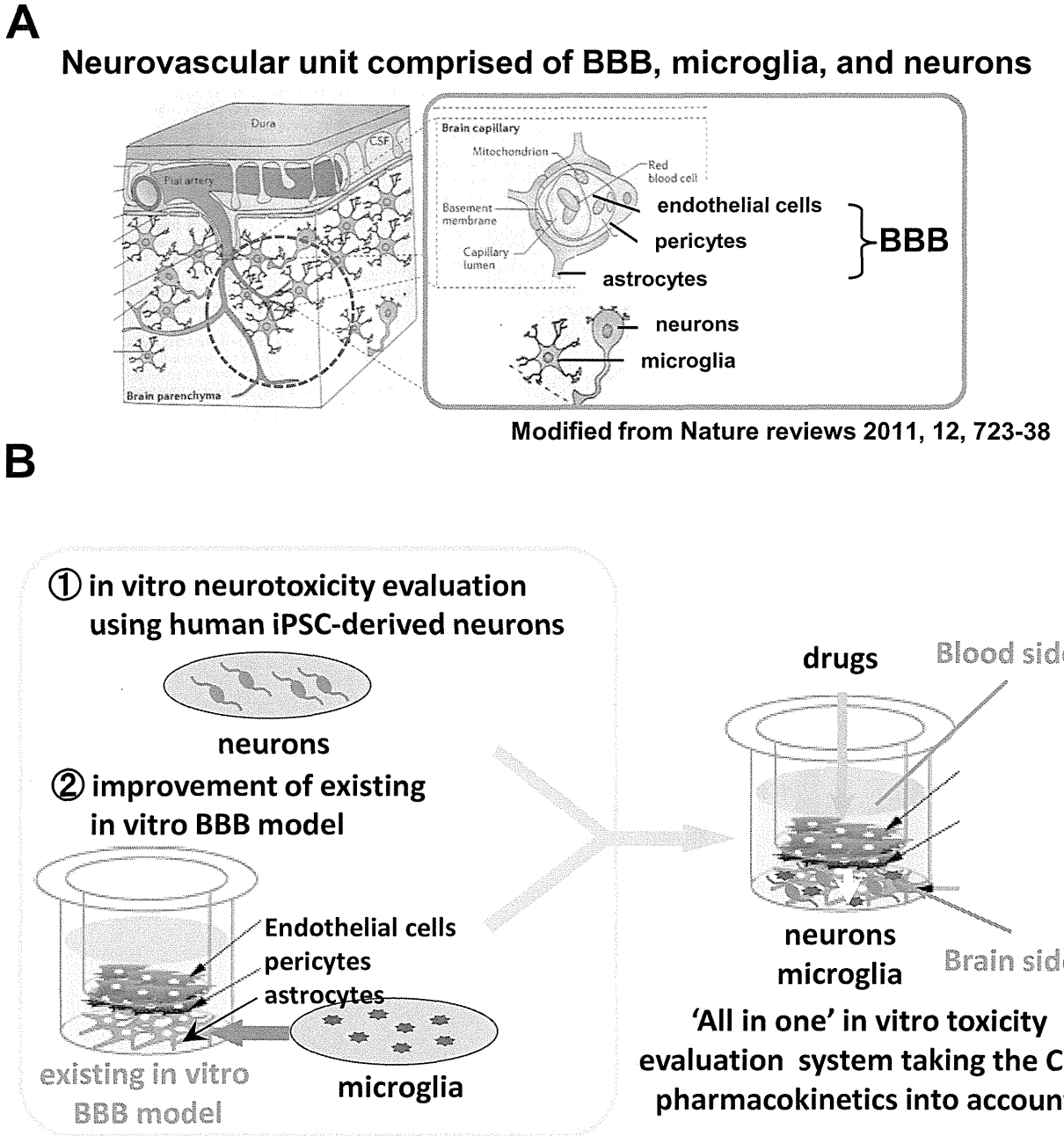

Fig. 1 The concept of our project

A. Neurovascular unit (NVU) is comprised of BBB, microglia, and neurons. Because drugs in the CNS reach neurons via BBB, the model system reproducing NVU is necessary to predict adverse effects on the CNS functions. **B.** We will establish the 'all in one' in vitro toxicity evaluation system taking the CNS pharmacokinetics into account.

Figure 2

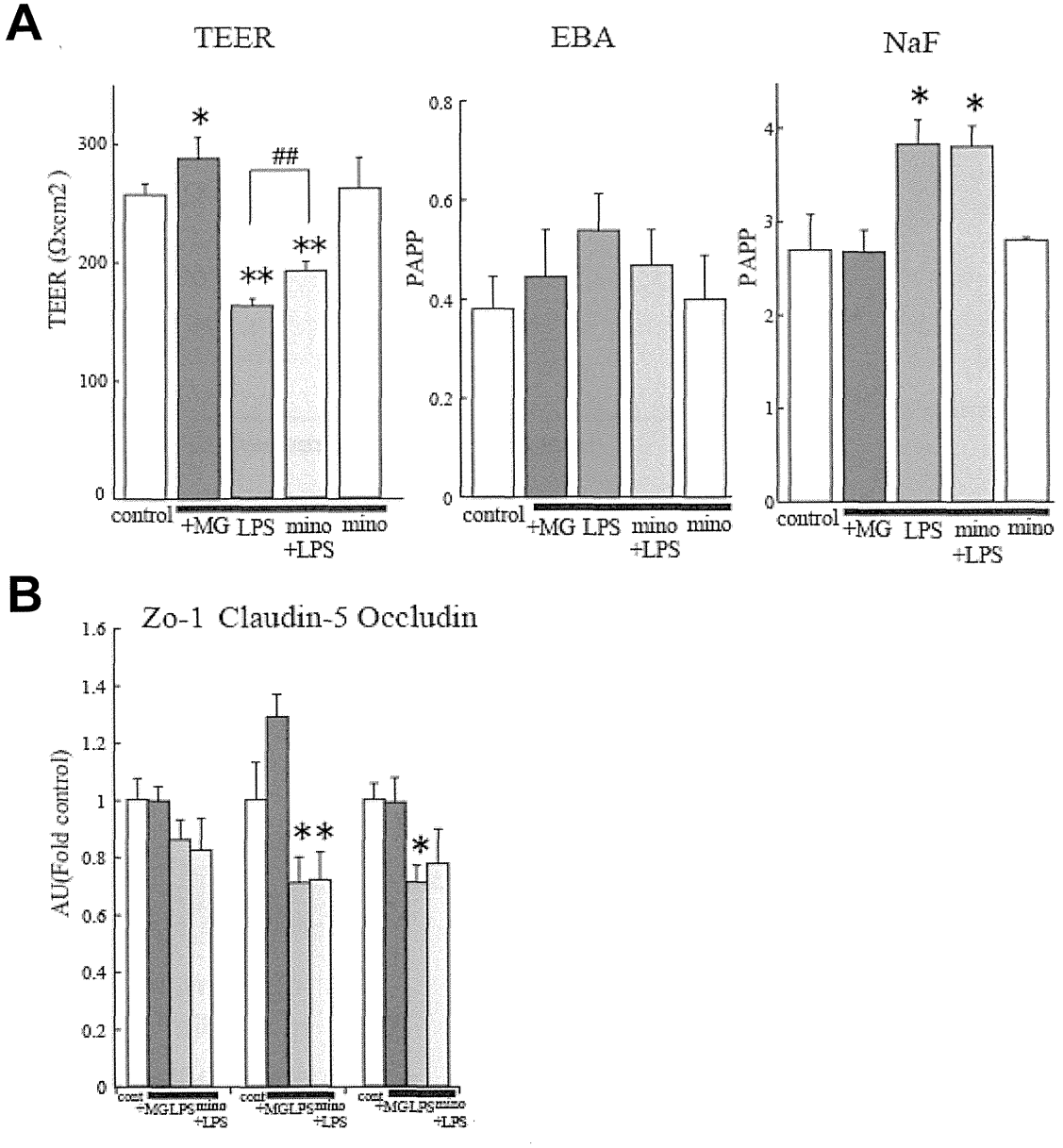

Fig. 2 Effects of LPS-activated microglia on the barrier function of BBB.

A. 4 day co-existence of LPS-activated microglia with astrocytes significantly decreased TEER, increased permeability of NaF of in vitro BBB model, whereas permeability of EBA remain unchanged.

B. LPS-activated microglia also decreased the expression level of Claudin5 and Occludin, which are important for the barrier function of BBB.

**:<0.01; *: <0.05 vs. control, ##: <0.01; #: <0.05 vs. +MG, by Tukey's test following ANOVA. Error bars represent s.e.m.

Figure 3

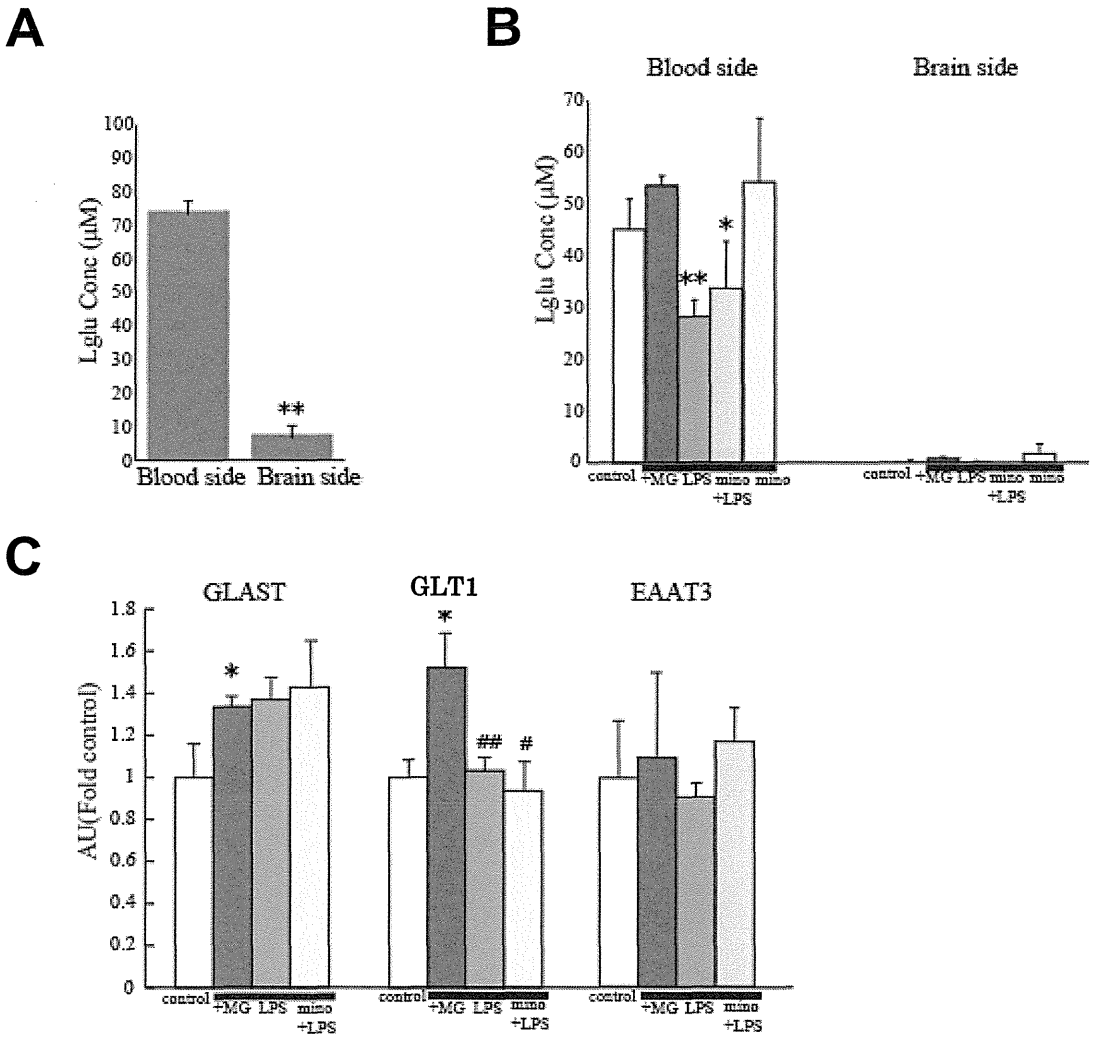

Fig. 3 Effects of LPS-activated microglia on the L-Glu transport activity of BBB.

A. After 5 day-incubation, L-Glu (50 μM at the start point) in the brain side was transported to the blood side.

B. In the presence of the activated-microglia, the increase in L-Glu in brain side was significantly suppressed.

C. Activated-microglia decreased the expression levels of GLT-1, but not GLAST and EAAT3.

**: <0.01; *: <0.05 vs. control, ##: <0.01; #: <0.05 vs. +MG, by Tukey's test following ANOVA. Error bars represent s.e.m.

Figure 4

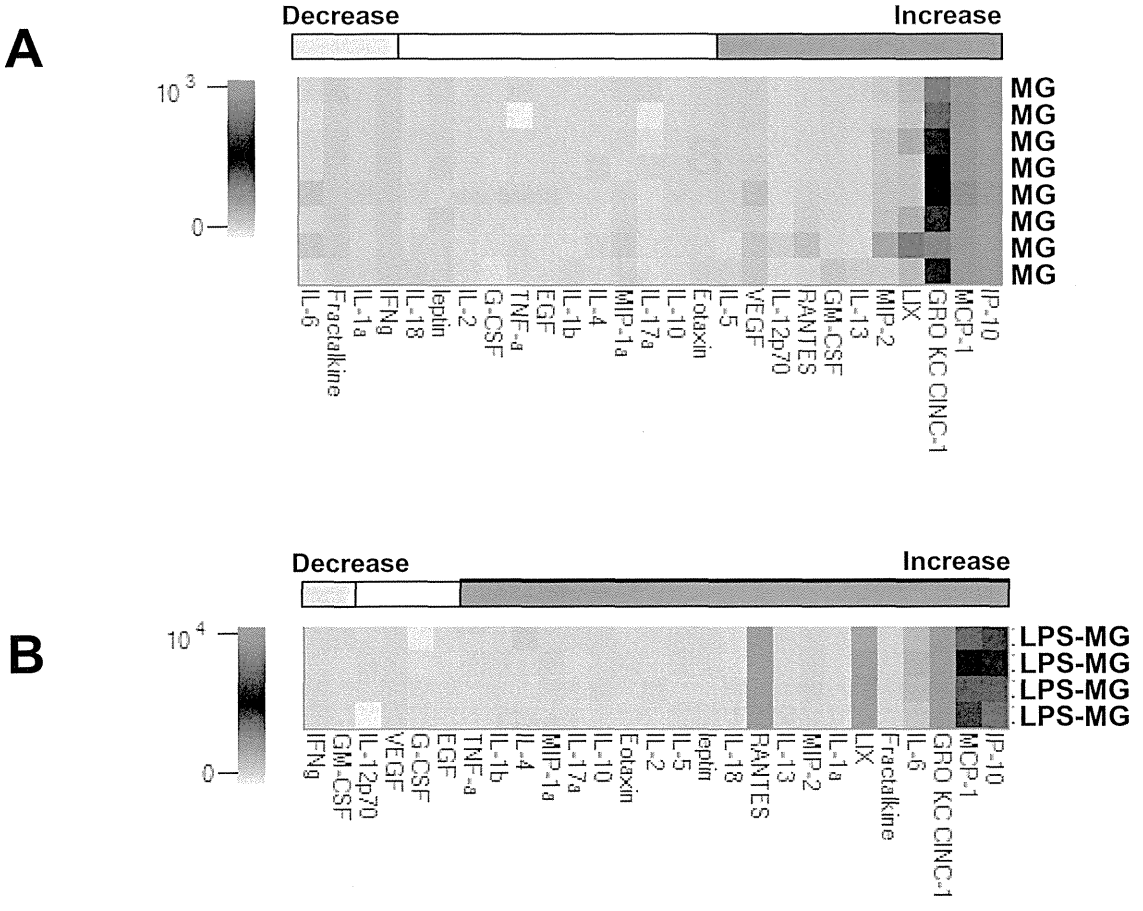

Fig. 4 The comprehensive quantitative analysis of cytokines and chemokines concentrations in the BBB culture supernatant.

A. 4 day co-existence of microglia with astrocytes significantly increased 11 chemokines and cytokines (VEGF, MCP-1, IP-10 etc.) and significantly decreased Fractalkine (vs. median of control group).

B. LPS-activated microglia significantly increased 18 chemokines and cytokines (RANTES, LIX, IL-6, GRO KC CINC-1, MCP-1, IP-10 etc.,).

The data shows as heatmap-graph analyzed by Milliplex analysis software.

別紙４

研究成果の刊行に関する一覧表

書籍

著者氏名	論文タイトル名	書籍全体の編集者名	書　籍　名	出版社名	出版地	出版年	ページ

雑誌

発表者氏名	論文タイトル名	発表誌名	巻号	ページ	出版年
Tashiro K, Hirata N, Okada A, Yamaguchi T, Takayama K, Mizuguchi H, **Kawabata K**.	Expression of coxsackievirus and adenovirus receptor separates hematopoietic and cardiac progenitor cells in Flk1-expressing mesoderm.	***Stem Cells Transl Med.***			in press
Okada A, Tashiro K, Yamaguchi T, **Kawabata K.**	Selective differentiation into hematopoietic and cardiac cells from pluripotent stem cells based on the expression of cell surface markers.	***Springer Protocol Methods in Molecular Biology ES Cells: Methods and Protocols- 2nd Edition.***			in press
Nagamoto Y, Takayama K, Tashiro K, Tateno C, Sakurai F, Tachibana M, **Kawabata K**, Ikeda K, Tanaka Y, Mizuguchi H.	Efficient engraftmentof human iPS cell-derived hepatocyte-like cells in uPA/SCID mice by overexpression of FNK, a Bcl-$x_L$mutant gene.	***Cell Transplant.***			in press
Takayama K, Morisaki Y, Kuno S, Nagamoto Y, Harada K, Furukawa N, Ohtaka M, Nishimura K, Imagawa K, Sakurai F, Tachibana M, Sumazaki R, Noguchi E, Nakanishi M, Hirata K, **Kawabata K**, Mizuguchi H.	Prediction of inter-individual differences in hepatic functions and drug sensitivity by using human iPS-derived hepatocytes.	***Proc. Natl. Acad. Sci. USA.***	47	16772-7	2014

Watanabe H, Takayama K, Inamura M, Tachibana M, Mimura N, Katayama K, Tashiro K, Nagamoto Y, Sakurai F, **Kawabata K**, Furue MK, Mizuguchi H.	HHEX promotes hepatic-lineage specification through the negative regulation of eomesodermin.	***PLoS One.***	3	e90791	2014
Tashiro K, Nonaka A, Hirata N, Yamaguchi T, Mizuguchi H, **Kawabata K**.	Plasma elevation of vascular endothelial growth factor leads to the reduction of mouse hematopoietic and mesenchymal stem/progenitor cells in the bone marrow.	***Stem Cells Dev.***	18	2202-2210	2014
Taura A, Furuta K, Yamaguchi T, **Kawabata K**, Tanaka S.	Regulation of histamine synthesis and tryptase expression through transcription factors, Gfi1 and Gfi1b, in murine cultured mast cells.	***Biol. Pharm. Bull.***	1	81-86	2014
Fujieda T, Koganezawa N, Ide Y, Shirao T, Sekino Y	An inhibitory pathway controlling the gating mechanism of the mouse lateral amygdala revealed by voltage-sensitive dye imaging.	***Neurosci Lett***	590C	126-31	2015
Mizui T, Sekino Y, Yamazaki Y, Ishizuka H, Takahashi H, Kojima N, Kojima M, Shirao T	Myosin II ATPase a ctivity mediates the long-term potentiatio n-induced exodus of stable F-actin bound by drebrin A from dendritic spines.	***PLoS One.***	9(1)	e8536722	2014
Shigemoto-Mogami Y, Hoshikawa K, Goldman JE, Sekino Y, Sato K	Microglia enhances neurogenesis and oligodendrogenesis in the early postnatal subventricular zone.	***J Neurosci***	34(5),	2231-43	2014
Nagakubo T, Demizu Y, Kanda Y, Misawa T, Shoda T, Okuhira K, Sekino Y, Naito M, Kurihara M	Development of Cell-Penetrating R7 Frag ment -Conjugated H elical Peptides as In hibitors of Estrogen Receptor-Mediated T ranscription.	***Bioconjug Chem***	25(11)	1921-24	2014

Hirata N, Yamada S, Shoda T, Kurihara M, **Sekino Y**, Kanda Y	Sphingosine-1-phosphate promotes expansion of cancer stem cells via S1PR3 by a ligand-independent Notch activation.	*Nat Commun*	5	4806	2014
Yamazaki H, Kojima N, Kato K, Hirose H, Iwasaki T, Mizui T, Takahashi H, Hanamura K, Roppongi RT, Koibuchi N, **Sekino Y**, Mori N, Shirao T	Spikar, a novel drebrin-binding protein, regulates the formation and stabilization of dendritic spines.	*J Neurochem*	128(4)	507-22	2014
Irie T, Matsuzaki Y, **Sekino Y**, Hirai H	Kv3.3 channels harboring a mutation of spinocerebellar ataxia type 13 alter excitability and induce cell death in cultured cerebellar Purkinje cells.	*J Physiol*	592(Pt 1) 34	229-47	2014
Fujimori K., Takaki J, Miura M, Shigemoto-Mogami Y, **Sekino Y**, Suzuki T, Sato K	Paroxetine prevented the down-regulation of astrocytic L-Glu transporters in neuroinflammation	*J Pharmacol Sci*			in press
Shigemoto-Mogami Y, Fujimori K, Ikarashi Y, Hirose A, **Sekino Y**, Sato K	Residual metals in carbon nanotubes suppress the proliferation of neural stem cells.	*Fundam Toxicol Sci*	1(3)	87-94	2014
Kim SR, Kubo T, Hojyo M, Matsuo T, Miyajima A, Usami M, **Sekino Y**, Matsushita T, Ishida S	Comparative metabolome analysis of cultured fetal and adult hepatocytes in human.	*J Toxicol Sci*	39(5)	717-23	2014
Yamada S, Kotake Y, Demizu Y, Kurihara Y, **Sekino Y**, Kanda Y	NAD-dependent isocitrate dehydrogenase as a novel target of tributyltin in human embryonic carcinoma cells.	*Sci Rep*	4	5952	2014

Nakamura Y, Matsuo J, Miyamoto N, Ojima A, Ando K, Kanda Y, Sawada K, Sugiyama A, Sekino Y	Assessment of testing methods for drug-induced repolarization delay and arrhythmias in an iPS cell-derived cardiomyocyte sheet: multi-site validation study.	*J Pharmacol Sci*	124(4)	494-501	2014
Ishikawa M, Shiota J, Ishibashi Y, Hakamata T, Shoji S, Fukuchi M, Tsuda M, Shirao T, Sekino Y. Baraban JM, Tabuchi A	Cellular localization and dendritic function of rat isoforms of the SRF coactivator MKL1 in cortical neurons.	*Neuroreport*	25(8)	585-92	2014

Prediction of interindividual differences in hepatic functions and drug sensitivity by using human iPS-derived hepatocytes

Kazuo Takayama[a,b,c], Yuta Morisaki[a], Shuichi Kuno[a], Yasuhito Nagamoto[a,c], Kazuo Harada[d], Norihisa Furukawa[a], Manami Ohtaka[e], Ken Nishimura[f], Kazuo Imagawa[a,c,g], Fuminori Sakurai[a,h], Masashi Tachibana[a], Ryo Sumazaki[g], Emiko Noguchi[i], Mahito Nakanishi[e], Kazumasa Hirata[d], Kenji Kawabata[j,k], and Hiroyuki Mizuguchi[a,b,c,l,1]

[a]Laboratory of Biochemistry and Molecular Biology; [b]iPS Cell-based Research Project on Hepatic Toxicity and Metabolism, [d]Laboratory of Applied Environmental Biology, [h]Laboratory of Regulatory Sciences for Oligonucleotide Therapeutics, Clinical Drug Development Project, and [k]Laboratory of Biomedical Innovation, Graduate School of Pharmaceutical Sciences, Osaka University, Osaka 565-0871, Japan; [c]Laboratory of Hepatocyte Regulation, and [j]Laboratory of Stem Cell Regulation, National Institute of Biomedical Innovation, Osaka 567-0085, Japan; [e]Research Center for Stem Cell Engineering, National Institute of Advanced Industrial Science and Technology, Ibaraki 305-8562, Japan; [f]Laboratory of Gene Regulation, [g]Department of Child Health, and [i]Department of Medical Genetics, Faculty of Medicine, University of Tsukuba, Ibaraki 305-8575, Japan; and [l]The Center for Advanced Medical Engineering and Informatics, Osaka University, Osaka 565-0871, Japan

Edited by Shinya Yamanaka, Kyoto University, Kyoto, Japan, and approved October 17, 2014 (received for review July 16, 2014)

Interindividual differences in hepatic metabolism, which are mainly due to genetic polymorphism in its gene, have a large influence on individual drug efficacy and adverse reaction. Hepatocyte-like cells (HLCs) differentiated from human induced pluripotent stem (iPS) cells have the potential to predict interindividual differences in drug metabolism capacity and drug response. However, it remains uncertain whether human iPSC-derived HLCs can reproduce the interindividual difference in hepatic metabolism and drug response. We found that cytochrome P450 (CYP) metabolism capacity and drug responsiveness of the primary human hepatocytes (PHH)-iPS-HLCs were highly correlated with those of PHHs, suggesting that the PHH-iPS-HLCs retained donor-specific CYP metabolism capacity and drug responsiveness. We also demonstrated that the interindividual differences, which are due to the diversity of individual SNPs in the CYP gene, could also be reproduced in PHH-iPS-HLCs. We succeeded in establishing, to our knowledge, the first PHH-iPS-HLC panel that reflects the interindividual differences of hepatic drug-metabolizing capacity and drug responsiveness.

human iPS cells | hepatocyte | CYP2D6 | personalized drug therapy | SNP

Drug-induced liver injury (DILI) is a leading cause of the withdrawal of drugs from the market. Human induced pluripotent stem cell (iPSC)-derived hepatocyte-like cells (HLCs) are expected to be useful for the prediction of DILI in the early phase of drug development. Many groups, including our own, have reported that the human iPS-HLCs have the ability to metabolize drugs, and thus these cells could be used to detect the cytotoxicity of drugs that are known to cause DILI (1, 2). However, to accurately predict DILI, it will be necessary to establish a panel of human iPS-HLCs that better represents the genetic variation of the human population because there are large interindividual differences in the drug metabolism capacity and drug responsiveness of hepatocytes (3). However, it remains unclear whether the drug metabolism capacity and drug responsiveness of human iPS-HLCs could reflect those of donor parental primary human hepatocytes (PHHs). To address this issue, we generated the HLCs differentiated from human iPSCs which had been established from PHHs (PHH-iPS-HLCs). Then, we compared the drug metabolism capacity and drug responsiveness of PHH-iPS-HLCs with those of their parental PHHs, which are genetically identical to the PHH-iPS-HLCs.

Interindividual differences of cytochrome P450 (CYP) metabolism capacity are closely related to genetic polymorphisms, especially single nucleotide polymorphisms (SNPs), in CYP genes (4). Among the various CYPs expressed in the liver, CYP2D6 is responsible for the metabolism of approximately a quarter of commercially used drugs and has the largest phenotypic variability, largely due to SNPs (5). It is known that certain alleles result in the poor metabolizer phenotype due to a decrease of CYP2D6 metabolism. Therefore, the appropriate dosage for drugs that are metabolized by CYP2D6, such as tamoxifen, varies widely among individuals (6). Indeed, in the 1980s, polymorphism in CYP2D6 appears to have contributed to the withdrawal of CYP2D6-metabolized drugs such as perhexiline from the market in many countries (7). If we could establish a panel of HLCs that better represents the diversity of genetic polymorphisms in the human population, it might be possible to determine the appropriate dosage of a drug for a particular individual. However, it is not known whether the drug metabolism capacity and drug responsiveness of HLCs reflect the genetic diversity, including SNPs, in CYP genes. Therefore, in this study we generated HLCs from several PHHs that have various SNPs on CYP2D6 and then compared the CYP2D6 metabolism capacity and responses to CYP2D6-metabolized drugs between the PHH-iPS-HLCs and parental PHHs.

Significance

We found that individual cytochrome P450 (CYP) metabolism capacity and drug sensitivity could be predicted by examining them in the primary human hepatocytes–human induced pluripotent stem cells–hepatocyte-like cells (PHH-iPS-HLCs). We also confirmed that interindividual differences of CYP metabolism capacity and drug responsiveness that are due to the diversity of individual single nucleotide polymorphisms in the CYP gene could also be reproduced in the PHH-iPS-HLCs. These findings suggest that interindividual differences in drug metabolism capacity and drug response could be predicted by using HLCs differentiated from human iPS cells. We believe that iPS-HLCs would be a powerful technology not only for accurate and efficient drug development, but also for personalized drug therapy.

Author contributions: K.T. and H.M. designed research; K.T., Y.M., and S.K. performed research; K.T., Y.M., Kazuo Harada, M.O., K.N., K.I., M.N., and Kazumasa Hirata contributed new reagents/analytic tools; K.T., Y.N., N.F., F.S., M.T., R.S., E.N., K.K., and H.M. analyzed data; and K.T. and H.M. wrote the paper.

The authors declare no conflict of interest.

This article is a PNAS Direct Submission.

Data deposition: The DNA microarray data reported in this paper have been deposited in the Gene Expression Omnibus (GEO) database, www.ncbi.nlm.nih.gov/geo (accession no. GSE61287).

[1]To whom correspondence should be addressed. Email: mizuguch@phs.osaka-u.ac.jp.

This article contains supporting information online at www.pnas.org/lookup/suppl/doi:10.1073/pnas.1413481111/-/DCSupplemental.

To this end, PHHs were reprogrammed into human iPSCs and then differentiated into the HLCs. To examine whether the HLCs could reproduce the characteristics of donor PHHs, we first compared the CYP metabolism capacity and response to a hepatotoxic drug between PHHs and genetically identical PHH-iPS-HLCs (12 donors were used in this study). Next, analyses of hepatic functions, including comparisons of the gene expression of liver-specific genes and CYPs, were performed to examine whether the hepatic characteristics of PHHs were reproduced in the HLCs. To the best of our knowledge, this is the first study to compare the functions between iPSC-derived cells from various donors and their parental cells with identical genetic backgrounds. Finally, we examined whether the PHH-iPS-HLCs exhibited a capacity for drug metabolism and drug responsiveness that reflect the genetic diversity such as SNPs on CYP genes.

Results

Reprogramming of PHHs to Human iPSCs. To examine whether the HLCs could reproduce interindividual differences in liver functions, we first tried to generate human iPSCs from the PHHs of 12 donors. PHHs were transduced with a Yamanaka 4 factor-expressing SeV (SeVdp-iPS) vector (*SI Appendix*, Fig. S1*A*) in the presence of SB431542, PD0325901, and a rock inhibitor, which could promote the somatic reprogramming (8). The reprogramming procedure is shown in *SI Appendix*, Fig. S1*B*. The human iPSCs generated from PHHs (PHH-iPSCs) were positive for alkaline phosphatase (*SI Appendix*, Fig. S1*B*, *Right*), NANOG, OCT4, SSEA4, SOX2, Tra1-81, and KLF4 (Fig. 1*A*). The gene expression levels of the pluripotent markers (*OCT3/4*, *SOX2*, and *NANOG*) in the PHH-iPSCs were approximately equal to those in human embryonic stem cells (ESCs) (*SI Appendix*, Fig. S1*C*, *Left*). The gene expression levels of the hepatic markers [*albumin (ALB)*, *CYP3A4*, and *αAT*] in the PHH-iPSCs were significantly lower than those in the parental PHHs (*SI Appendix*, Fig. S1*C*, *Right*). We also confirmed that the PHH-iPSCs have the ability to differentiate into the three embryonic germ layers in vitro by embryoid body formation and in vivo by teratoma formation (*SI Appendix*, Fig. S2 *A* and *B*, respectively). To verify that the PHH-iPSCs originated from PHHs, short tandem repeat analysis was performed in the PHH-iPSCs and parental PHHs (*SI Appendix*, Fig. S2*C*). The results showed that the PHH-iPSCs were indeed originated from PHHs. Taken together, these results indicated that the generation of human iPSCs from PHHs was successfully performed. It is known that a transient epigenetic memory of the original cells is retained in early-passage iPSCs, but not in late-passage iPSCs (9). To examine whether the hepatic differentiation capacity of PHH-iPSCs depends on their passage number, PHH-iPSCs having various passage numbers were differentiated into the hepatic lineage (Fig. 1*B*). The *tyrosine aminotransferase* (*TAT*) expression levels and albumin (ALB) secretion levels in early passage PHH-iPS-HLCs (fewer than 10 passages) were higher than those of late passage PHH-iPS-HLCs (more than 14 passages). These results suggest that the hepatic differentiation tendency is maintained in early passage PHH-iPSCs, but not in late passage PHH-iPSCs. In addition, the hepatic functions of late passage PHH-iPS-HLCs were similar to those in the HLCs derived from late passage non–PHH-derived iPS cells (such as dermal cells, blood cells, and Human Umbilical Vein Endothelial Cells (HUVEC)-derived iPS cells) (*SI Appendix*, Fig. S3). Therefore, PHH-iPSCs, which were passaged more than 20 times, were used in our study to avoid any potential effect of transient epigenetic memory retained in parental PHHs on hepatic functions.

HLCs Were Differentiated from PHH-iPSCs Independent of Their Differentiation Tendency. To compare the hepatic characteristics among the PHH-iPS-HLCs that were generated from PHHs of

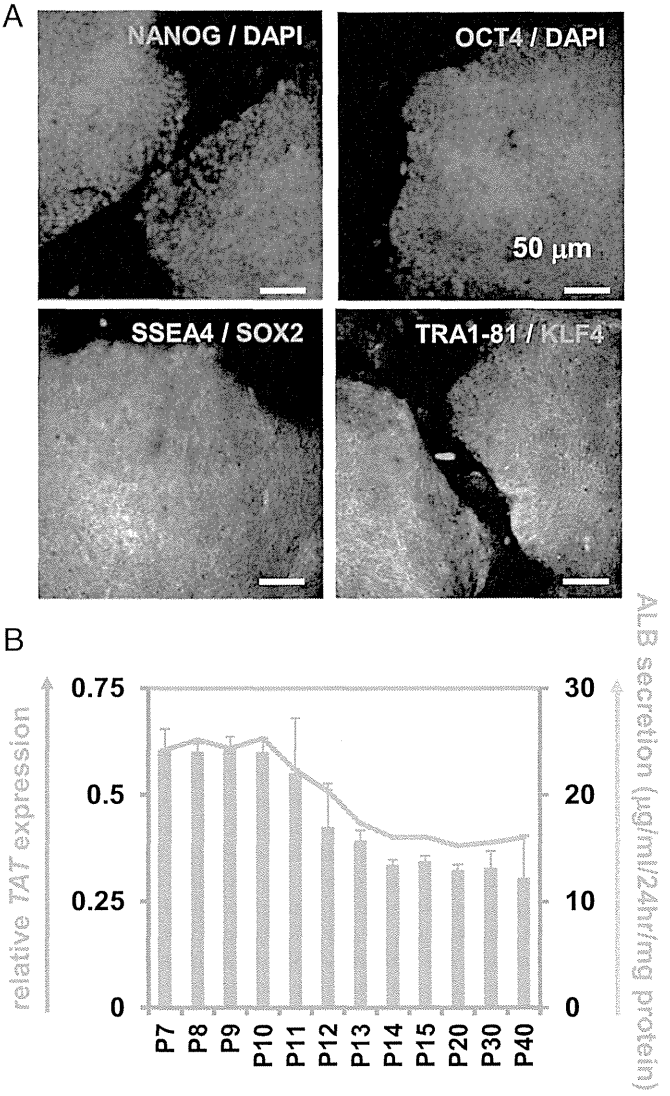

Fig. 1. Establishment and characterization of human iPSCs generated from PHHs. (*A*) The PHH-iPSCs were subjected to immunostaining with anti-NANOG (red), OCT4 (red), SSEA4 (green), SOX2 (red), TRA1-81 (green), and KLF4 (red) antibodies. Nuclei were counterstained with DAPI (blue) (*Upper*). (*B*) The *TAT* expression and ALB secretion levels in the PHH-iPS-HLCs (P7–P40) were examined. On the *y* axis, the gene expression level of *TAT* in PHHs was taken as 1.0.

the 12 donors, all of the PHH-iPSCs were differentiated into the HLCs as described in Fig. 2*A*. However, the differences in hepatic function among PHH-iPS-HLCs could not be properly compared because there were large inter-PHH-iPSC line differences in the hepatic differentiation efficiency based on ALB or asialoglycoprotein receptor 1 (ASGR1) expression analysis (Fig. 2*B*). In addition, there were also large inter-PHH-iPS-HLC line differences in ALB or urea secretion capacities (Fig. 2*C*). These results suggest that it is impossible to compare the hepatic characteristics among PHH-iPS-HLCs without compensating for the differences in the hepatic differentiation efficiency. Recently, we developed a method to maintain and proliferate the hepatoblast-like cells (HBCs) generated from human ESCs/iPSCs by using human laminin 111 (LN111) (10). To examine whether the hepatic differentiation efficiency could be made uniform by generating the HLCs following purification and proliferation of the HBCs, the PHH-iPS-HBCs were cultured on LN111 as

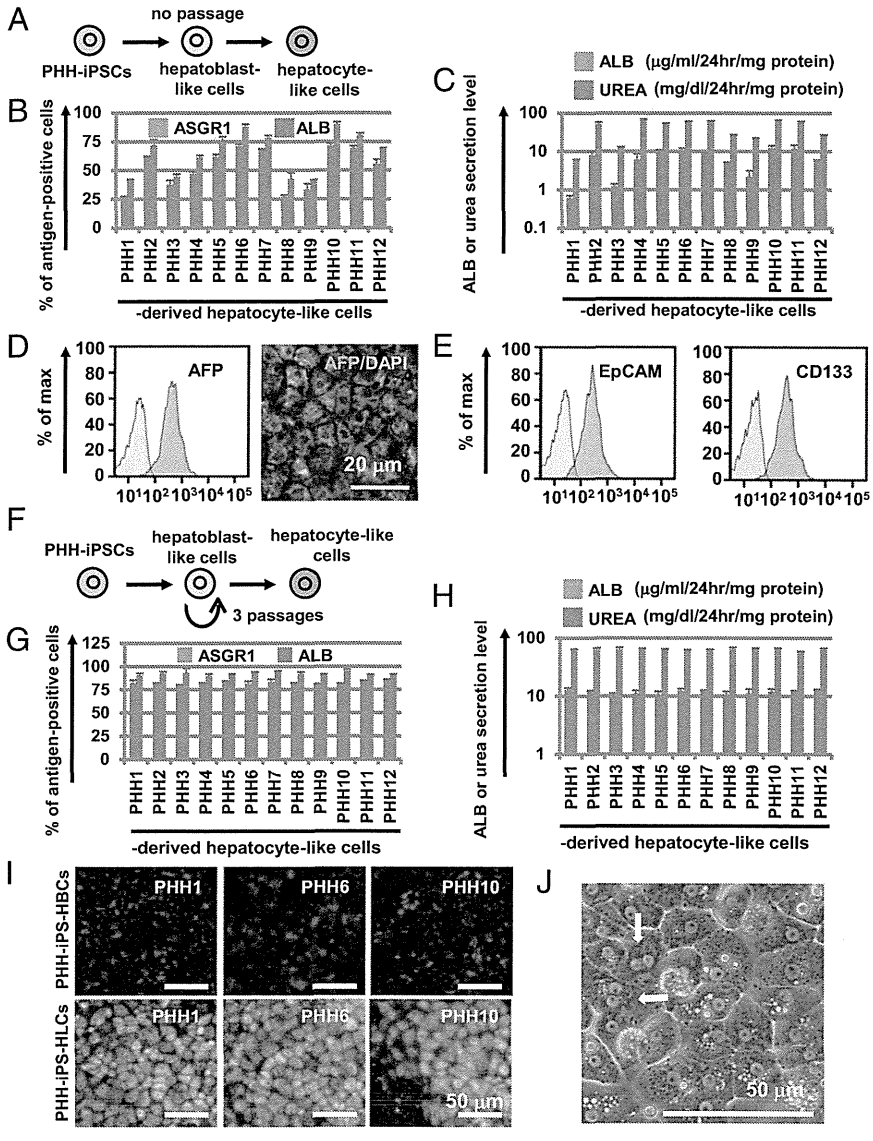

Fig. 2. Highly efficient hepatocyte differentiation from PHH-iPSCs independent of their differentiation tendency. (*A*) PHH-iPSCs were differentiated into the HLCs via the HBCs. (*B*) On day 25 of differentiation, the efficiency of hepatocyte differentiation was measured by estimating the percentage of ASGR1- or ALB-positive cells using FACS analysis. (*C*) The amount of ALB or urea secretion was examined in PHH-iPS-HLCs. (*D*) The percentage of AFP-positive cells in PHH-iPS-HBCs was examined by using FACS analysis (*Left*). The PHH-iPS-HBCs were subjected to immunostaining with anti-AFP (green) antibodies. Nuclei were counterstained with DAPI (blue) (*Right*). (*E*) The percentage of EpCAM- and CD133-positive cells in PHH-iPS-HBCs was examined by using FACS analysis (*Left*). (*F*) PHH-iPSCs were differentiated into the hepatic lineage, and then PHH-iPS-HBCs were purified and maintained for three passages on human LN111. Thereafter, expanded PHH-iPS-HBCs were differentiated into the HLCs. (*G*) The efficiency of hepatic differentiation from PHH-iPS-HBCs was measured by estimating the percentage of ASGR1- or ALB-positive cells using FACS analysis. (*H*) The amount of ALB or urea secretion in PHH-iPS-HLCs was examined. Data represent the mean ± SD from three independent differentiations. (*I*) The PHH1-, 6-, or 10-iPS-HBCs and -HLCs were subjected to immunostaining with anti-αAT (green) antibodies. Nuclei were counterstained with DAPI (blue). (*J*) A phase-contrast micrograph of PHH-iPS-HLCs.

previously described (10), and then differentiated into the HLCs. Almost all of the cells were positive for the hepatoblast marker [alpha-fetoprotein (AFP)] (Fig. 2*D*). In addition, the PHH-iPS-HBCs were positive for two other hepatoblast markers, EpCAM and CD133 (Fig. 2*E*). To examine the hepatic differentiation efficiency of the PHH-iPS-HBCs maintained on LN111-coated dishes for three passages (Fig. 2*F*), the HBCs were differentiated into the HLCs, and then the percentage of ALB- and ASGR1-positive cells was measured by FACS analysis (Fig. 2*G*). All 12 PHH-iPS-HBCs could efficiently differentiate into the HLCs, yielding more than 75% or 85% ASGR1- or ALB-positive cells, respectively. In addition, there was little difference between the PHH-iPSC lines in ALB or urea secretion capacities (Fig. 2*H*). Although there were large differences in the hepatic differentiation capacity among the PHH1/6/10 (Fig. 2*B*), PHH1/6/10-iPS-HBCs could efficiently differentiate into the HLCs that homogeneously expressed αAT (Fig. 2*I*). After the hepatic differentiation of the PHH-iPS-HBCs, the morphology of the HLCs was similar to that of the PHHs: polygonal with distinct round binuclei (Fig. 2*J*). These results indicated that the hepatic differentiation efficiency of the 12 PHH-iPSC lines could be rendered uniform by inducing hepatic maturation after the establishment of self-renewing HBCs. Therefore, we expected that differences in the hepatic characteristics among the HLCs generated from the 12 individual donor PHH-iPS-HBCs could be properly compared. In addition, the hepatic differentiation efficiency could be rendered uniform not only in the PHH-iPSC lines but also in non–PHH-iPSC lines and human ESCs by performing hepatic maturation after the establishment of self-renewing HBCs (*SI Appendix*, Fig. S4). In Figs. 3 and 4, the HLCs were differentiated after the HBC proliferation step to normalize the hepatic differentiation efficiency.

PHH-iPS-HLCs Retained Donor-Specific Drug Metabolism Capacity and Drug Responsiveness. To examine whether the hepatic functions of individual PHH-iPS-HLCs reflect those of individual PHHs, the CYP metabolism capacity and drug responsiveness of PHH-iPS-HLCs were compared with those of PHHs. PHHs are often used as a positive control to assess the hepatic functions of the HLCs, although in all of the previous reports, the donor of PHHs has been different from that of human iPSCs. Because it is generally considered that CYP activity differs widely among individuals, the hepatic functions of the HLCs should be compared with those of genetically identical PHHs to accurately evaluate the hepatic functions of the HLCs. The CYP1A2, -2C9, and -3A4 activity levels in the PHH-iPS-HLCs were ~60% of

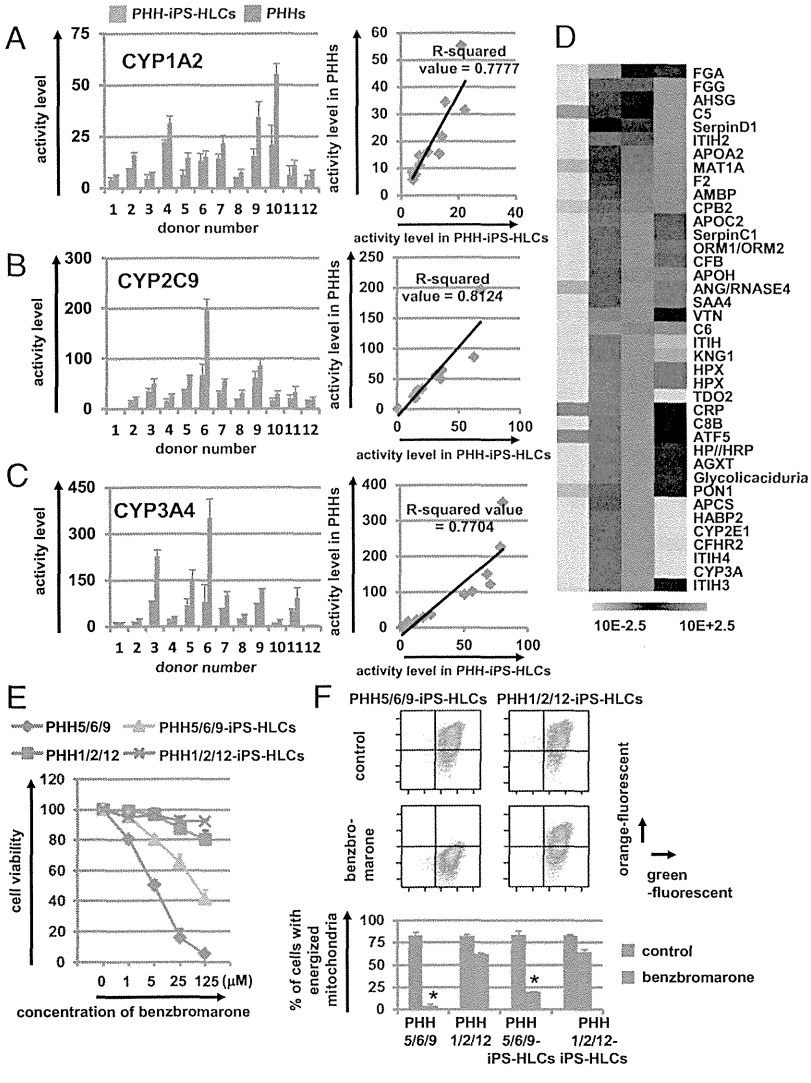

Fig. 3. The drug metabolism capacity and drug responsiveness of PHH-iPS-HLCs were highly correlated with those of their parental PHHs. (*A*–*C*) CYP1A2 (*A*), -2C9 (*B*), and -3A4 (*C*) activity levels in PHH-iPS-HLCs and PHHs were measured by LC-MS/MS analysis. The R-squared values are indicated in each figure. (*D*) The global gene expression analysis was performed in PHH9-iPSCs, PHH9-iPS-HLCs, PHH9s, and HepG2 (PHH-iPSCs, PHH-iPS-HLCs, and PHHs are genetically identical). Heat-map analyses of liver-specific genes are shown. (*E*) The cell viability of PHH5/6/9, PHH1/2/12, PHH5/6/9-iPS-HLCs, and PHH1/2/12-iPS-HLCs was examined after 24 h exposure to different concentrations of benzbromarone. The cell viability was expressed as a percentage of that in the cells treated only with solvent. (*F*) The percentage of cells with energized mitochondria in the DMSO-treated (control, *Upper*) or benzbromarone-treated (*Lower*) cells based on FACS analysis. Double-positive cells (green+/orange+) represent energized cells, whereas single-positive cells (green+/orange–) represent apoptotic and necrotic cells. Data represent the mean ± SD from three independent experiments (*Lower Graph*). Student *t* test indicated that the percentages in the "control" were significantly higher than those in the "benzbromarone" group ($P < 0.01$). The "PHH5/6/9" represents the average value of cell viability (*E*) or mitochondrial membrane potential (*F*) in PHH5, PHH6, and PHH9. The "PHH1/2/12" represents the average value of cell viability or mitochondrial membrane potential in PHH1, PHH2, and PHH12. PHH5, PHH6, and PHH9 were the top three with respect to CYP2C9 activity levels, whereas PHH1, PHH2, and PHH12 had the lowest CYP2C9 activity levels.

those in the PHHs (Fig. 3 *A*–*C* and *SI Appendix*, Fig. S5). Interestingly, the CYP1A2, -2C9, and -3A4 activity levels in the PHH-iPS-HLCs were highly correlated with those in the PHHs (the R-squared values were more than 0.77) (Fig. 3 *A*, *B*, and *C*, respectively). These results suggest that it would be possible to predict the individual CYP activity levels through analysis of the CYP activity levels of the PHH-iPS-HLCs. Because the average and variance of CYP3A4 activity levels in PHH-iPS-HLCs, non–PHH-iPS-HLCs, and human ES-HLCs were similar to each other (*SI Appendix*, Fig. S6), the drug metabolism capacity of PHH-iPS-HLCs might be similar to that of nonliver tissue-derived iPS-HLCs and human ES-HLCs. Therefore, it might be possible to predict the diversity of drug metabolism capacity among donors by using nonliver tissue-derived iPS-HLCs and human ES-HLCs as well as PHH-iPS-HLCs. On the other hand, the CYP induction capacities of PHH-iPS-HLCs were weakly correlated with those of PHHs (*SI Appendix*, Fig. S7 *A*–*C*). To further investigate the characteristics of the HLCs, DNA microarray analyses were performed in genetically identical undifferentiated iPSCs, PHH-iPS-HLCs, and PHHs. The gene expression patterns of liver-specific genes, CYPs, and transporters in the PHH-iPS-HLCs were similar to those in PHHs (Fig. 3*D* and *SI Appendix*, Fig. S7 *D* and *E*, respectively). Next, the hepatotoxic drug responsiveness of PHH-iPS-HLCs was compared with that of PHHs. Benzbromarone, which is known to cause hepatotoxicity by CYP2C9 metabolism (11), was treated to PHH5/6/9 and PHH5/6/9-iPS-HLCs, which have high CYP2C9 activity, or PHH1/2/12 and PHH1/2/12-iPS-HLCs which have low CYP2C9 activity (Fig. 3*E*). The susceptibility of the PHH5/6/9 and PHH5/6/9-iPS-HLCs to benzbromarone was higher than that of PHH1/2/12 and PHH1/2/12-iPS-HLCs, respectively. These results were attributed to the higher CYP2C9 activity levels in PHH5/6/9 and PHH5/6/9-iPS-HLCs compared with those in PHH1/2/12 and PHH1/2/12-iPS-HLCs. Because it is also known that benzbromarone causes mitochondrial toxicity (12), an assay of mitochondrial membrane potential was performed in benzbromarone-treated PHHs and PHH-iPS-HLCs (Fig. 3*F*). The mitochondrial toxicity observed in PHH5/6/9 and PHH5/6/9-iPS-HLCs was more severe than that in PHH1/2/12 and PHH1/2/12-iPS-HLCs, respectively. Taken together, these results suggest that the hepatic functions of the individual PHH-iPS-HLCs were highly correlated with those of individual PHHs.

Interindividual Differences in CYP2D6-Mediated Metabolism and Drug Toxicity, Which Are Caused by SNPs in CYP2D6, Are Reproduced in the PHH-iPS-HLCs. Because certain SNPs are known to have a large impact on CYP activity, the genetic variability of CYP plays an important role in interindividual differences in drug response. CYP2D6 shows the large phenotypic variability due to genetic polymorphism (13). We next examined whether the PHHs used

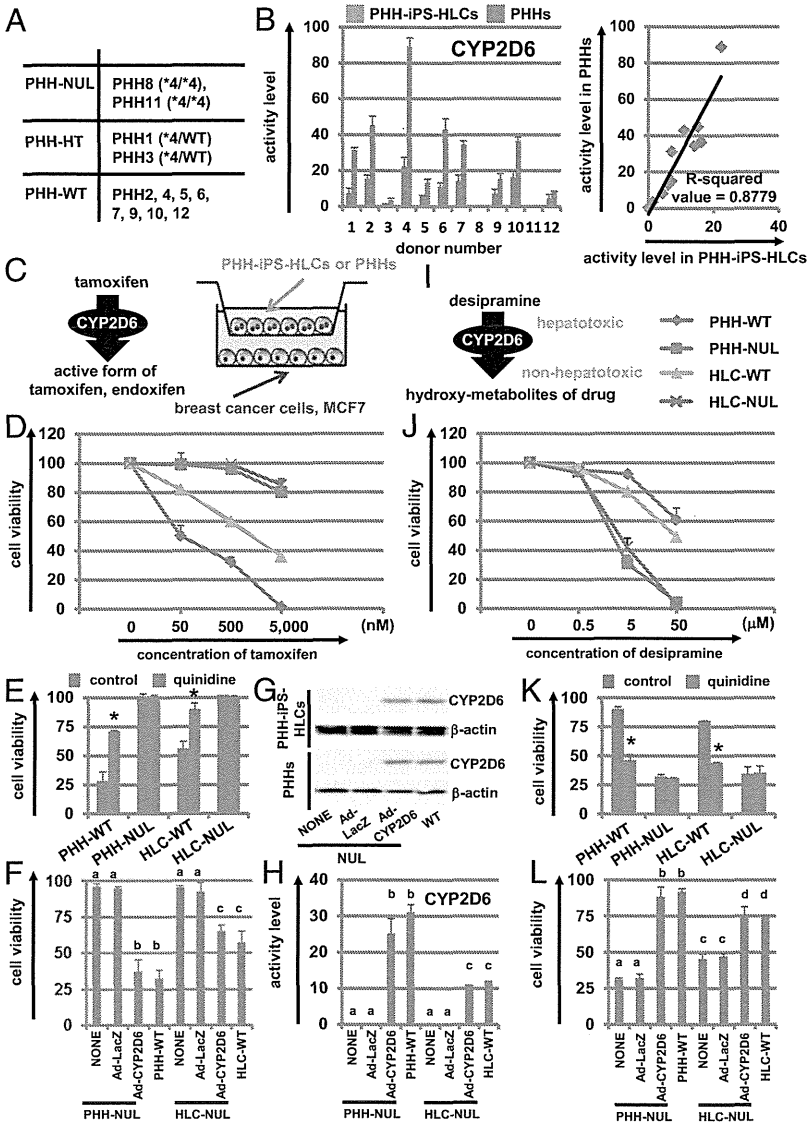

Fig. 4. The interindividual differences in CYP2D6 metabolism capacity and drug responsiveness induced by SNPs in CYP2D6 are reproduced in the PHH-iPS-HLCs. (*A*) SNPs (CYP2D6*3, *4, *5, *6, *7, *8, *16, and *21) in the CYP2D6 gene were analyzed. (*B*) The CYP2D6 activity levels in PHH-iPS-HLCs and PHHs were measured by LC-MS/MS analysis. (*C*) The pharmacological activity of tamoxifen-dependent conversion to its metabolite, endoxifen, by the CYP2D6. The coculture system of breast cancer cells (MCF-7 cells) and the PHH-iPS-HLCs are illustrated. (*D*) The cell viability of MCF-7 cells was assessed after 72-h exposure to different concentrations of tamoxifen. (*E*) The cell viability of MCF-7 cells, which were cocultured with PHH-WT, PHH-NUL, HLC-WT, and HLC-NUL, was assessed after 72-h exposure to 500 nM of tamoxifen in the presence or absence of 3 nM quinidine (a CYP2D6 inhibitor). (*F*) The cell viability of MCF-7 cells cocultured with Ad-CYP2D6-transduced PHH-NUL and HLC-NUL was examined after 72-h exposure to 500 nM of tamoxifen. (*G* and *H*) The CYP2D6 expression (*G*) and activity (*H*) levels in Ad-CYP2D6-transduced PHH-NUL and HLC-NUL were examined by Western blotting and LC-MS/MS analysis. (*I*) The detoxification of desipramine-dependent conversion to its conjugated form by the CYP2D6. (*J*) The cell viability of PHH-WT, PHH-NUL, HLC-WT, and HLC-NUL was assessed after 24-h exposure to different concentrations of desipramine. (*K*) The cell viability of the PHH-WT and HLC-WT was assessed after 24-h exposure to 5 μM of desipramine in the presence or absence of 5 μM of quinidine (a CYP2D6 inhibitor). (*L*) The cell viability of the Ad-CYP2D6-transduced PHH-NUL and HLC-NUL was examined after 24-h exposure to 5 μM of desipramine. The cell viability was expressed as a percentage of that in the cells treated with only solvent. Data represent the mean ± SD from three independent experiments. In *E* and *K*, Student *t* test indicated that the cell viability in the "control" was significantly higher than that in the "quinidine" group ($P < 0.01$). In *F*, *H*, and *L*, statistical significance was evaluated by ANOVA followed by Bonferroni post hoc tests to compare all groups. Groups that do not share the same letter are significantly different from each other ($P < 0.05$).

in this study have the CYP2D6 poor metabolizer genotypes (CYP2D6 *3, *4, *5, *6, *7, *8, *16, and *21) (5). PHH8 and -11 have CYP2D6*4 (null allele), whereas the others have a wild type (WT) or hetero allele (*SI Appendix*, Table S3 and Fig. 4*A*). Consistent with this finding, the PHH8/11-iPS-HLCs also have CYP2D6*4, whereas the others have a wild type or hetero allele. As expected, the CYP2D6 activity levels in the PHH8/11 (PHH-NUL) and PHH8/11-iPS-HLC (HLC-NUL) were significantly lower than those in the PHH-WT and HLC-WT, respectively (Fig. 4*B*). The pharmacological activity of tamoxifen, which is the most widely used agent for patients with breast cancer, is dependent on its conversion to its metabolite, endoxifen, by the CYP2D6 (Fig. 4*C*). To examine whether the pharmacological activity of tamoxifen could be predicted by using PHHs and HLCs that have either the null type CYP2D6*4 allele or wild-type CYP2D6 allele, the breast cancer cell line MCF7 was cocultured with PHHs or HLCs, and then the cells were treated with tamoxifen (Fig. 4*D*). The cell viability of MCF7 cells cocultured with PHHs-NUL or HLCs-NUL was significantly higher than that of MCF7 cells cocultured with PHHs-WT or HLCs-WT. The decrease in cell viability of MCF7 cells cocultured with PHHs-WT or HLCs-WT was rescued by treatment with a CYP2D6 inhibitor, quinidine (Fig. 4*E*). We also confirmed that the cell viability of MCF7 cells cocultured with PHHs-NUL or HLCs-NUL was decreased by CYP2D6 overexpression in the PHHs-NUL or HLCs-NUL (Fig. 4*F*). Note that the expression (Fig. 4*G*) and activity (Fig. 4*H*) levels of CYP2D6 in CYP2D6-expressing adenovirus vector (Ad-CYP2D6)-transduced PHHs-NUL or HLCs-NUL were comparable to those of PHHs-WT or HLCs-WT. These results indicated that the PHHs-WT and HLCs-WT could more efficiently metabolize tamoxifen than the PHHs-NUL and HLCs-NUL, respectively, and thereby induced higher toxicity in MCF7 cells. Similar results were obtained with the other breast cancer cell line, T-47D (*SI Appendix*, Fig. S8 *A–D*). Next, we examined whether the CYP2D6-mediated drug-induced hepatotoxicity could be predicted by using PHHs and HLCs having either a null type CYP2D6*4 allele or wild-type CYP2D6 allele. PHHs and HLCs were treated with desipramine, which is known to cause hepatotoxicity (Fig. 4*I*) (14). The cell viability of PHHs-NUL and HLCs-NUL was significantly lower than that of PHHs-WT and HLCs-WT (Fig. 4*J*). The cell viability of the PHHs-WT or HLCs-WT was decreased by treatment with a CYP2D6 inhibitor, quinidine (Fig. 4*K*). We also confirmed that the decrease in the cell viability of the PHHs-NUL or HLCs-NUL was rescued by CYP2D6 overexpression in the PHHs-NUL or HLCs-NUL (Fig. 4*L*). Similar

results were obtained with the other hepatotoxic drug, perhexiline (*SI Appendix*, Fig. S8 *E–H*). These results indicated that the PHHs-WT and HLCs-WT could more efficiently metabolize imipramine and thereby reduce toxicity compared with the PHHs-NUL and HLCs-NUL. Taken together, our findings showed that the interindividual differences in CYP metabolism capacity and drug responsiveness, which are prescribed by an SNP in genes encoding CYPs, were also reproduced in the PHH-iPS-HLCs.

Discussion

The purpose of this study was to examine whether the individual HLCs could reproduce the hepatic function of individual PHHs. A Yamanaka 4 factor-expressing SeV vector was used in this study to generate integration-free human iPSCs from PHHs. It is known that SeV vectors can express exogenous genes without chromosomal insertion, because these vectors replicate their genomes exclusively in the cytoplasm (15). To examine the different cellular phenotypes associated with SNPs in human iPSC derivatives, the use of integration-free human iPSCs is essential.

We found that the CYP activity levels of the PHH-iPS-HLCs reflected those of parent PHHs, as shown in Fig. 3 *A–C*. There were few interindividual differences in the ratio of CYP expression levels in the PHH-iPS-HLCs to those in PHHs (*SI Appendix*, Fig. S5). Together, these results suggest that it is possible to predict the individual CYP activity levels through analysis of the CYP activity levels of the PHH-iPS-HLCs. In the future, it will be necessary to confirm these results in skin or blood cell-derived iPSCs as well as PHH-iPSCs, although donor-matched PHHs and blood cells (or skin cells) are difficult to obtain. In addition, the comparison of hepatic functions between genetically identical PHHs and PHH-iPS-HLCs (Fig. 3 *A–C*) would enable us to accurately ascertain whether the HLCs exhibit sufficient hepatic function to be a suitable substitute for PHHs in the early phase of pharmaceutical development. Because the drug responsiveness of the individual HLCs reflected that of individual PHHs (Fig. 3 *E* and *F*), it might be possible to perform personalized drug therapy following drug screening using a patient's HLCs. However, the R-squared values of the individual CYP activities differed from each other (Fig. 3 *A–C*), suggesting that the activity levels of some CYPs are largely influenced not only by genetic information but also by environmental factors, such as dietary or smoking habits.

The interindividual differences of CYP2D6 metabolism capacity and drug responsiveness that were prescribed by SNP in genes encoding CYP2D6 were reproduced in the PHH-iPS-HLCs (Fig. 4). It was impossible to perform drug screening in the human hepatocytes derived from a donor with rare SNPs because these hepatocytes could not be obtained. However, because human iPSCs can be generated from such donors with rare SNPs, the CYP metabolism capacity and drug responsiveness of these donors might be possible to predict. Further, it would also be possible to identify the novel SNP responsible for an unexpected hepatotoxicity by using the HLCs in which whole genome sequences are known. We thus believe that the HLCs will be a powerful tool not only for accurate and efficient drug development but also for personalized drug therapy.

Experimental Procedures

DNA Microarray. Total RNA was prepared from the PHH9-iPSCs, PHH9-iPS-HLCs, PHH9, and human hepatocellular carcinoma cell lines by using an RNeasy Mini kit. A pool of three independent samples was used in this study. cRNA amplifying, labeling, hybridizing, and analyzing were performed at Miltenyi Biotec. The Gene Expression Omnibus (GEO) accession no. for the microarray analysis is GSE61287.

Flow Cytometry. Single-cell suspensions of human iPSC-derived cells were fixed with 2% (vol/vol) paraformaldehyde (PFA) for 20 min, and then incubated with the primary antibody (described in *SI Appendix*, Table S1), followed by the secondary antibody (described in *SI Appendix*, Table S2). In case of the intracellular staining, the Permeabilization Buffer (eBioscience) was used to create holes in the membrane thereby allowing the antibodies to enter the cell effectively. Flow cytometry analysis was performed using a FACS LSR Fortessa flow cytometer (BD Biosciences).

ACKNOWLEDGMENTS. We thank Yasuko Hagihara, Natsumi Mimura, and Shigemi Isoyama for their excellent technical support. H.M. and K.K. were supported by grants from the Ministry of Health, Labor, and Welfare. H.M. was also supported by the Project for Technological Development, Research Center Network for Realization of Regenerative Medicine of the Japan Science and Technology Agency and by the Uehara Memorial Foundation. F.S. was supported by the Program for Promotion of Fundamental Studies in Health Sciences of the National Institute of Biomedical Innovation. K.T. and Y.N. were supported by a grant-in-aid for the Japan Society for the Promotion of Science Fellows.

1. Takayama K, et al. (2012) Efficient generation of functional hepatocytes from human embryonic stem cells and induced pluripotent stem cells by HNF4α transduction. *Mol Ther* 20(1):127–137.
2. Medine CN, et al. (2013) Developing high-fidelity hepatotoxicity models from pluripotent stem cells. *Stem Cells Transl Med* 2(7):505–509.
3. Ingelman-Sundberg M (2004) Pharmacogenetics of cytochrome P450 and its applications in drug therapy: The past, present and future. *Trends Pharmacol Sci* 25(4): 193–200.
4. Ingelman-Sundberg M (2001) Genetic susceptibility to adverse effects of drugs and environmental toxicants. The role of the CYP family of enzymes. *Mutat Res* 482(1-2): 11–19.
5. Zhou SF (2009) Polymorphism of human cytochrome P450 2D6 and its clinical significance: Part I. *Clin Pharmacokinet* 48(11):689–723.
6. Borges S, et al. (2006) Quantitative effect of CYP2D6 genotype and inhibitors on tamoxifen metabolism: Implication for optimization of breast cancer treatment. *Clin Pharmacol Ther* 80(1):61–74.
7. Bakke OM, Manocchia M, de Abajo F, Kaitin KI, Lasagna L (1995) Drug safety discontinuations in the United Kingdom, the United States, and Spain from 1974 through 1993: A regulatory perspective. *Clin Pharmacol Ther* 58(1):108–117.
8. Lin T, et al. (2009) A chemical platform for improved induction of human iPSCs. *Nat Methods* 6(11):805–808.
9. Polo JM, et al. (2010) Cell type of origin influences the molecular and functional properties of mouse induced pluripotent stem cells. *Nat Biotechnol* 28(8):848–855.
10. Takayama K, et al. (2013) Long-term self-renewal of human ES/iPS-derived hepatoblast-like cells on human laminin 111-coated dishes. *Stem Cell Reports* 1(4):322–335.
11. McDonald MG, Rettie AE (2007) Sequential metabolism and bioactivation of the hepatotoxin benzbromarone: Formation of glutathione adducts from a catechol intermediate. *Chem Res Toxicol* 20(12):1833–1842.
12. Kaufmann P, et al. (2005) Mechanisms of benzarone and benzbromarone-induced hepatic toxicity. *Hepatology* 41(4):925–935.
13. Ingelman-Sundberg M (2005) Genetic polymorphisms of cytochrome P450 2D6 (CYP2D6): Clinical consequences, evolutionary aspects and functional diversity. *Pharmacogenomics J* 5(1):6–13.
14. Spina E, et al. (1997) Relationship between plasma desipramine levels, CYP2D6 phenotype and clinical response to desipramine: A prospective study. *Eur J Clin Pharmacol* 51(5):395–398.
15. Nishimura K, et al. (2011) Development of defective and persistent Sendai virus vector: A unique gene delivery/expression system ideal for cell reprogramming. *J Biol Chem* 286(6):4760–4771.